Fluid Flow and Heat Transfer Characteristics in Triangular Grooved Microchannel Heat Sinks with the Same Volume

[1]Cui Yang and [2]Zhu Qifeng,

[1,2]Henan Polytechnic University, School of Mechanical and Power Engineering, Jiaozuo, China

Abstract-Four groups of microchannel heat sinks with equal-volume triangular grooves were designed, and the effects of groove geometry and arrangement on the flow and heat transfer characteristics of microchannels were numerically studied. The results show that the mixing of hot and cold fluids caused by the grooves not only increases the flow resistance of the microchannel, but also enhances the heat transfer. When the channel volume is the same, the flow resistance and heat transfer of the microchannel increase with the increase of grooves depth and the decrease of grooves width. For the same grooves, the flow resistance and Nusselt number of the microchannels with aligned grooves are larger than those of the microchannels with offset ones. The overall performance, the heat transfer entropy production and the entropy production of the microchannels increase with the increase of the groove width, and the maximum of the enhanced heat transfer factor can be achieved up to 1.42.

Keywords-*Microchannel heat sink; Triangular groove; Heat transfer enhancement; Entropy; Arrangement*

I. INTRODUCTION

With the development of the electronics industry, a single electronic equipment due to a large number of transistors gathered and high frequency work, produce huge heat, resulting in a rise in temperature, and then affect the reliability of the equipment, serious will cause major safety accidents. Therefore, the heat sink with small volume and high heat dissipation efficiency is urgently needed to meet the heat dissipation requirements of high calorific electronic equipment.

In 1981 Tuckerman and Pease[1] proposed a water-cooled integrated micro-channel cooling system, which has the characteristics of small volume and high heat transfer efficiency, and has attracted extensive attention from researchers at home and abroad. The researchers explored the cooling performance of smooth rectangular cross section microchannels under different heat flow conditions and proposed a variety of methods to optimize and improve their overall performance.Wang et al.[2]studied the influence of geometric parameters on the flow and heat transfer characteristics of rectangular, trapezoidal and triangular cross section microchannels through numerical simulation.Yue et al.[3] found that as the volume fraction of nanoparticles increased, the number of Nusselt and pump power increased, and the total entropy production decreased.

In order to further improve the heat transfer performance of micro-channel heat sink, Ahmed et al.[4] proposed a micro-channel with cavities arranged on the side wall of the flow channel. It was found that when the Reynolds number was 100, the trapeze groove type micro-channel had the best heat transfer enhancement performance, and the Nusselt number increased by 51.59%.Zhu et al.[5]explored the influence of groove shape on the flow and heat transfer characteristics of the microchannel, and found that the surface microchannel of the

triangular groove had the best comprehensive performance. Danish et al.[6] studied the thermal resistance and pump power characteristics of micro-channel radiators and found that micro-channel with groove wall could obtain lower thermal resistance and higher Nussert number. The groove structure of the side wall reduces the thickness of the thermal boundary layer, increases the convective heat transfer area, and improves the heat transfer performance while reducing the pressure drop[7].Xia et al.[8] studied the effects of biased fan-shaped grooves and triangular grooves on the flow and heat dissipation performance of microchannels, and pointed out that heat transfer enhancement can be attributed to the injection and throttling effects and the enhancement of fluid disturbance.Steinke and Kandlikard[9] made a comprehensive review of the friction coefficient data of liquid flow in microchannels, and pointed out that the loss of inlet and outlet should be considered.

It can be seen from the literature review above that the groove surface microchannel has better heat transfer performance and lower flow pressure drop.However, the current research mainly focuses on the influence of groove shape and geometric parameters on flow and heat transfer, and there is a lack of comprehensive exploration of the flow mechanism in groove microchannels.In this paper, a series of micro-channel heat sink models with the same flow volume were designed based on the triangular groove geometry. The influences of groove geometry size and arrangement on flow and heat transfer characteristics of micro-channel were analyzed, and the internal reasons of groove surface reducing flow resistance of micro-channel and enhancing heat transfer characteristics were explored.

II. NUMERICAL MODEL

A. Microchannel geometry model

In this paper, four groups of equal-volume triangular grooves are designed, and eight microchannel heat sink models are constructed by means of opposite row (MC-ATR) and staggered row (MC-OTR).In order to save computing resources, based on the symmetry of the microchannel heat sink model, a channel, half solids on both sides and the corresponding matrix at the bottom are selected as the computational domain of numerical simulation, as shown in Fig. 1.The length (L_{com}), width (W_{com}) and height (H_{com}) of the calculation domain are 10 mm, 0.3mm and 0.35mm, respectively. The width (W_c) and height (H_c) of the fluid domain are 0.1mm and 0.2mm, respectively. The triangular grooves are arranged on the wall surface on both sides of the flow passage in the way of alignment and cross-alignment. The microchannel triangular groove period (S_g) is fixed at 0.8mm.There are four groups of geometric parameters for triangular grooves, with widths (W_g) and depths (H_g) of 0.2 and 0.06mm, 0.3 and 0.04mm, 0.4 and 0.03mm, and 0.6 and 0.02mm, respectively.
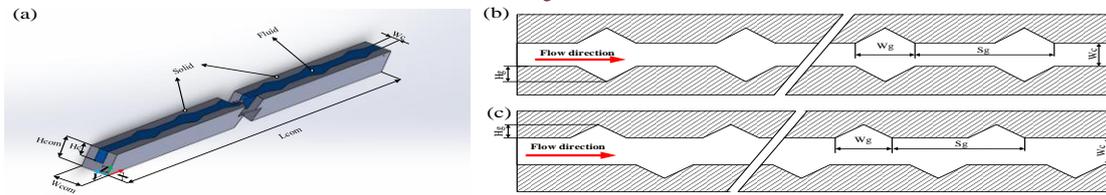
Figure 1: Calculation domain of microchannel heat sink

B. Mathematical model

Shah et al.[10] pointed out that if the Knudsen value (Kn) is less than 10-3, the fluid can be considered continuous. Kn of microchannel heat sink in this paper is much less than 10-3. Therefore, it can be assumed that the liquid flow inside the microchannel is continuous. The fluid flow in the microchannel is steady laminar flow, and the influence of surface tension, gravity, viscous dissipation and radiation heat transfer can be ignored. The microchannel substrate is silicon with fixed thermal properties. The flowing working medium is deionized water, and the thermal physical parameters change with temperature[11].

Based on the above assumptions, the governing equation of the micro-channel three-dimensional fluid-structure coupling heat transfer numerical model can be simplified into the following form:

Continuity Equation:

$$\nabla V = 0 \tag{1}$$

Momentum Equation:

$$\rho_f (V \cdot \nabla V) = -\nabla p + \nabla(\mu_f \cdot \nabla V) \tag{2}$$

Energy equation in the fluid domain:

$$\rho_f C_{Pf} V \cdot \nabla T_f = \nabla(k_f \cdot \nabla T_f) \tag{3}$$

Energy equation in the solid domain:

$$\nabla(k_s \cdot \nabla T_s) = 0 \tag{4}$$

V is the velocity vector of the fluid, m/s; p is the pressure, Pa; ρf fluid density, Kg/m3; Cp,ffor specific heat at constant pressure of fluid, kJ/(Kg·K); μ f dynamic viscosity coefficient, Pa s.; kfand ks are the thermal conductivity of fluid and solid, W/(m·K); Tfand Tsare the temperature of fluid and solid matrix respectively, K.

The boundary conditions of microchannel simulation are as follows: (1) the fluid temperature at the entrance of the microchannel is Tin=298K, and the velocity vector is perpendicular to the entrance of the microchannel; (2) Microchannel outlet pressure p_{out}=0Pa; (3) The two sides are symmetric boundaries; (4) The bottom surface is constant heat flux, q_w=10⁶W/m²; (5) The fluid-solid contact surface is a thermal coupling boundary; (6) The remaining surfaces are adiabatic boundaries.

C. Computational grid

ANSYS FlUENT18.1 was used to solve the numerical model of microchannel flow and heat transfer. The pressure-velocity field is decoupled by SIMPLEC algorithm, and the governing equation is discretized by a second-order upwind scheme to obtain faster convergence and computational accuracy. The residual difference of each physical quantity is set to 10-6.

In order to select the optimal number of grids and balance the calculation accuracy and calculation cost, taking micro-channel MC-ATR3 as an example, error analysis was carried out on the numerical calculation results under different grids. The relative error calculation formula is as follows:

$$e\% = \left| \frac{M_1 - M}{M_1} \right| \times 100\% \tag{5}$$

In the formula, M is the calculation result of different grids, and M1 is the calculation result of 1.272 million grids. When Re=430, Tab. 1 lists the friction coefficient, average Nusselt number and relative error of microchannel heat sink obtained with different mesh numbers. It can be seen that when the mesh number is 703,000, the friction coefficient deviation is 1.98% and the average Nusselt number deviation is 0.11%, which can meet the accuracy requirements of the calculation results.

Table 1:Grid Independence Verification

Grid Quantity (million)	f	Et(%)	Nu	Et(%)
0.234	0.109	7.92%	9.41	5.26%
0.401	0.106	4.95%	9.20	2.91%
0.703	0.103	1.98%	8.95	0.11%
1.272	0.101	-	8.94	-

III. PERFORMANCE EVALUATION

The formula for calculating Reynolds number is as follows:

$$Re = \rho_f u_m D_h / \mu_f \tag{6}$$

u_m is the average velocity of the fluid, m/s; Dh is the hydraulic diameter of the channel, m. Hydraulic diameter formula is as follows:

$$D_h = \frac{2 H_c W_c}{H_c + W_c} \tag{7}$$

the height and width of Hcand Wcchannels respectively, m.

The formula for calculating liquid flow pressure drop in the microchannel is as follows:

$$\Delta p = p_{in} - p_{out} \tag{8}$$

p_{in} is the inlet pressure of the channel; kPa.

The formula of average friction coefficient is as follows:

$$f = \frac{2 D_h \Delta p}{L_{com} \rho_f u^2} \tag{9}$$

The formula of average heat transfer coefficient is as follows:

A_h is the heating surface area, m2; A_{con} is the area of fluid-structure coupling surface, m2; T_W is the mean temperature of the fluid-structure coupling surface, K; T_f is the mean temperature of the fluid, K.

$$h = \frac{q_w A_h}{A_{con}(T_W - T_f)} \tag{10}$$

The formula for the average Nusselt number is as follows:

$$Nu = hD_h / k_f \tag{11}$$

In order to be able to have a better comparison of liquidity and heat transfer performance of micro channel with smooth channel, Webb[12] presented for dimensional parameters, such as strengthening η to evaluate the comprehensive performance of microchannel heat transfer factor, the formula as below:

$$\eta = \frac{Nu / Nu_0}{(f / f_0)^{1/3}} \tag{12}$$

Nu_0 and f_0 are the average Nusselt number and average friction coefficient of rectangular smooth microchannels respectively.

Bejan[13] proposed that volume entropy yield was used to calculate the entropy yield of the microchannel, which consisted of irreversible loss caused by flow friction and irreversible loss caused by heat transfer, namely:

$$\dot{S}_{gen} = \dot{S}_{gen,\Delta T} + \dot{S}_{gen,\Delta P} \tag{13}$$

$$\dot{S}_{gen,\Delta P} = \iiint_\Omega \dot{S}_{gen,\Delta P} dV = \frac{m}{\rho T_f} \Delta p \tag{14}$$

$$\dot{S}_{gen,\Delta T} = \iiint_\Omega \dot{S}_{gen,\Delta T} dV = \frac{q A_b (T_w - T_f)}{T_f T_w} \tag{15}$$

$$N_{s,a} = \dot{S}_{gen} / \dot{S}_{gen,0} \tag{16}$$

$\dot{S}_{gen,0}$ for the smooth passage of the total entropy production.

IV. REFINE RESULTS

A. Model verification

In order to verify the reliability of the numerical model, the numerical simulation results of the rectangular smooth microchannel were compared with the theoretical calculation results, as shown in Figure 2. The maximum relative errors of the theoretical and simulated results from the microchannel friction factor[14] and the inlet and outlet temperature difference[15] are 7.3% and 1.5%, respectively.
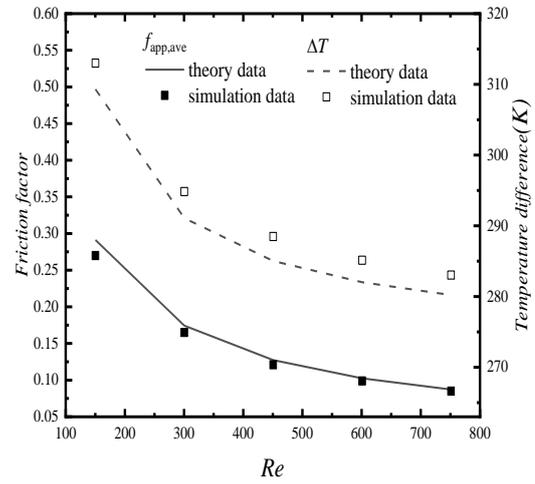

Figure 2: Validation of numerical model

B. Structure of hot fluid flow field

Shown in Fig.3 and Fig.4, respectively Re =430 different microchannel heat sink was perpendicular to the x-y section (z = 0.175 mm、4.0<x<5.6 mm) on the velocity and temperature distribution in the cloud.The fluid flow velocity is the fastest at the center of the microchannel, the slowest at the side wall of the microchannel, and the fluid flow velocity decreases at the groove due to the increase of the cross-sectional area. The streamline in the microchannel on the surface of the groove is deflected at the groove and tends to the inside of the groove.The grooves of MC-ATR1, MC-OTR1, MC-ATR2 and MC-OTR2 formed obvious local flow vortices opposite to the main stream, which seriously hindered heat transfer.As the depth of the groove decreases and the width increases, the scale of the vortex in the groove becomes smaller and smaller until it disappears. When the size of triangular grooves is the same, vortex is more likely to form in the microchannel of contralateral grooves, while periodic wave-like bending flow occurs in the contralateral grooves microchannel.
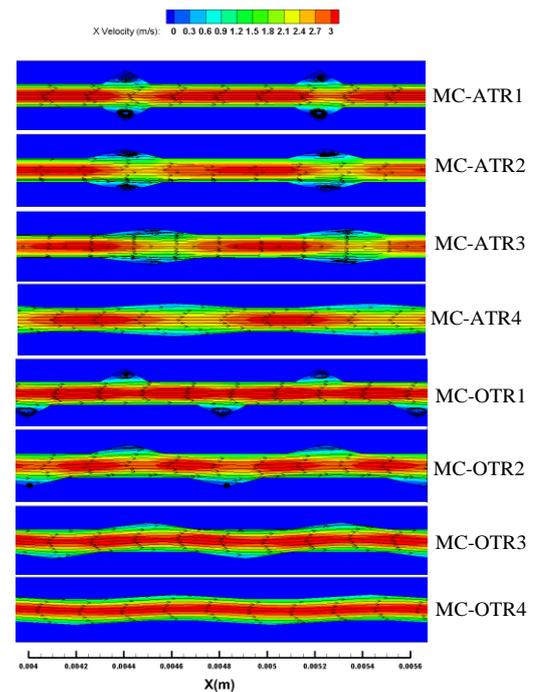

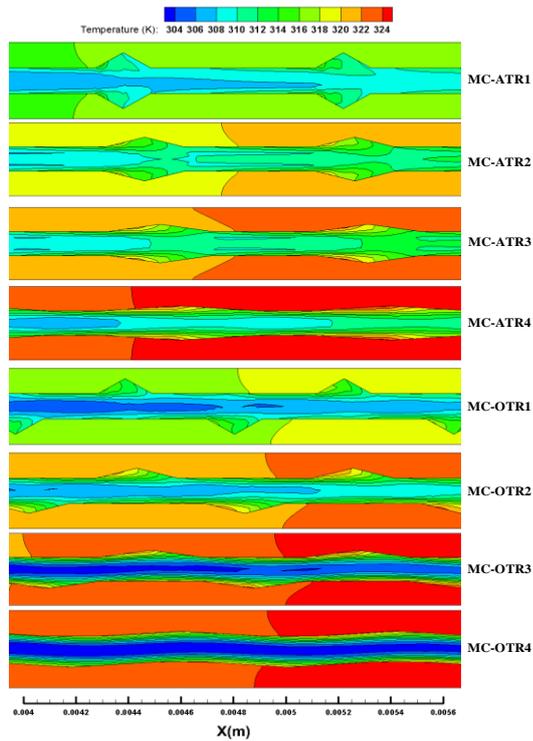Figure 3: z=0.175mm section velocity nebulae distribution

Figure 4:Local temperature nebulae distribution on the section
z=0.175mm

As can be seen from Fig.4, continuous and stable thickened thermal boundary layer cannot be formed in the micro-channel on the surface of the groove, and the thermal boundary layer is interrupted at the groove.The temperature in the expansion section of the leading edge of the groove is higher than that in the contraction section of the trailing edge, because the injection fluid has more obvious scour effect on the contraction section of the trailing edge of the groove, and the heat transfer performance is more prominent, so the wall temperature is lower.On the one hand, the temperature of the expansion section of the groove front is higher because the fluid has weak scour effect on the wall surface. On the other hand, the reverse vortex in the groove absorbs the heat of the groove wall, and the fluid temperature rises.There are wavy-like flows in the staggered triangular groove microchannel, and the fluid ejection effect is weak, so the disturbance to the thermal boundary layer is small. When the geometry of the triangular groove is the same, the heat transfer performance is better than that of the staggered triangular groove microchannel.

C. Flow and heat transfer properties

Fig. 5 and Fig. 6 respectively show the changes of flow pressure drop and relative friction coefficient at the inlet and outlet of different microchannels. The pressure drop and friction coefficient of microchannel increase with the increase of Re.At high Re, the difference of pressure drop between microchannels is obvious, and the effect of fluid inertia force is enhanced. The geometry and arrangement of triangular grooves have an important effect on fluid flow.When Re =717, the pressure drop of MC-ATR4 decreased by 33.38 kPa compared with MC-ATR1. The pressure drop of MC-OTR4 is 31.45 kPa lower than that of MC-OTR1.When the geometry of triangular grooves is the same, the flow pressure drop of triangular grooves in the opposite row is greater than that of corresponding staggered grooves. This is because the sudden expansion of grooves caused by the opposite row is far greater than that of staggered grooves, so the fluid ejection effect is stronger than that of

staggered grooves, resulting in greater flow resistance. When Re = 717, the maximum f/f0 of MC-ATR1 channel reaches 1.32.
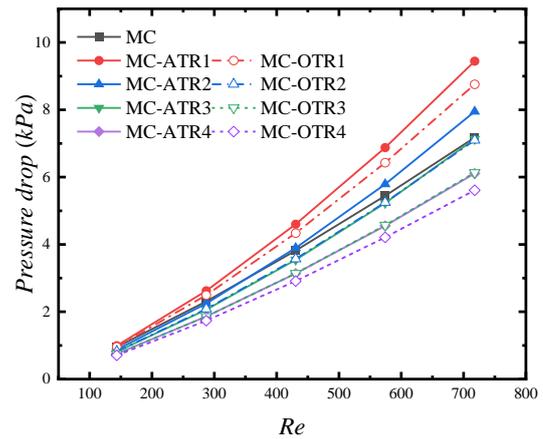

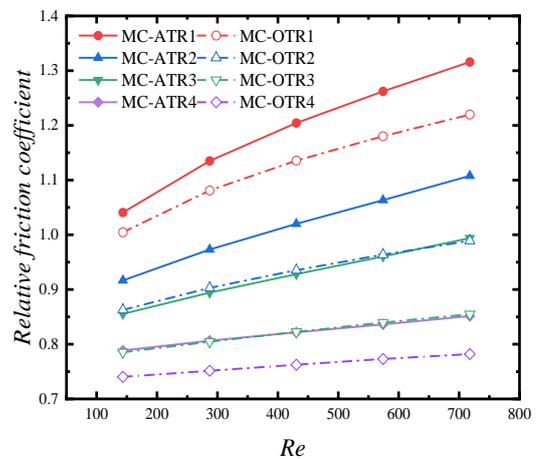Figure 5: Change in flow pressure drop

Figure 6: Change in relative friction coefficient

Fig. 7 shows the changes of the average temperature of the heating surface at the bottom of different microchannels along the flow direction. Along the flow direction, the temperature of the heating surface gradually rises, because the fluid in the channel absorbs heat along the flow direction, the temperature gradually rises, the temperature difference between the fluid and the solid becomes smaller, and the heat transfer performance decreases.MC-ATR1 has the lowest temperature, while MC-ATR4 has the highest temperature. When x is less than 0.005m, the temperature of MC-ATR4 is higher than that of the smooth surface microchannel; otherwise, it is lower than that of the smooth surface microchannel, and the average temperature of other microchannels is lower than that of the smooth surface microchannel.In the groove arrangement mode, the temperature of MC-ATR4 is higher than that of MC-OTR4, and the heating surface temperature of the microchannel on the surface of the opposite groove is lower than that on the surface of the staggered groove in other microchannels.

Fig. 8 shows the variation characteristics of the relative Nusselt number of different microchannels. The Nusselt number of microchannels increases with the increase of Reynolds number, which is because the convective heat transfer ability is enhanced with the increase of flow velocity.MC-ATR1 has the largest Nusser-number, while MC-OTR4 has the smallest Nusser-number.This is because the flow channel of MC-ATR1 in the groove has the largest expansion degree, the strongest injection effect, the strongest mixing degree of hot and cold

fluids, and the best heat transfer performance.The Nusselt number of allocated-groove microchannels is greater than that of staggered microchannels.When Reynolds number is less than 500, the Nusselt number of MC-ATR4 and MC-OTR4 is smaller than that of smooth surface microchannel, because the fluted structure disturbs the fluid in the channel weakly at low Reynolds number, and the convective heat transfer performance decreases. When Re=717, the maximum Nu/Nu_0 of MC-ATR1 channel is 1.55.
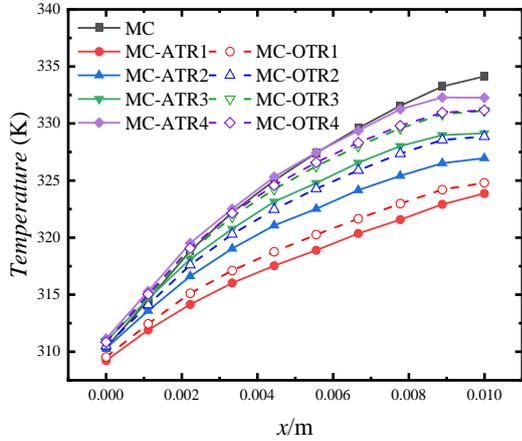

Figure 7:Change in the mean temperature of the heating surface
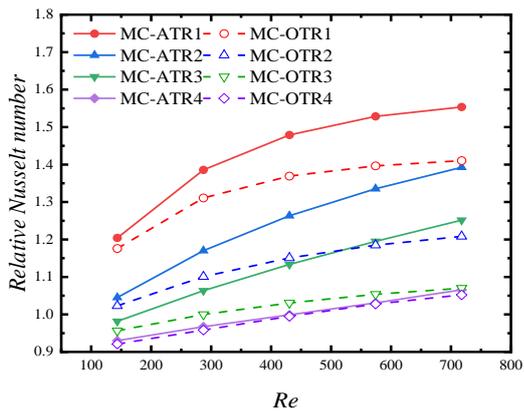

Figure 8:The change in the relative Nusselt number

Fig. 9 shows for the triangular groove surface to strengthen the microchannel flow and heat transfer performance of heat transfer factor (η) changes. The greater the value of ηmeans for the comprehensive performance of microchannel, the better.Can be seen from the figure in the grooves on the surface of the strengthening of the microchannel heat transfer factor η increased with the increase of Re, but at high Reynolds number, ηincrease rate decreases.When the geometry of triangular groove is the same, the maximum value of enhanced heat transfer factor differs by 10% in different arrangements. MC-ATR1 has the best comprehensive performance, and its comprehensive enhanced heat transfer factor reaches 1.42 when Re=717.The comprehensive performance of MC-ATR4 channel is the worst, and its maximum enhanced heat transfer factor is only 1.01.On the whole, the comprehensive performance of the contralateral triangular groove microchannel is higher than that of the staggered triangular groove microchannel. However, when the groove depth is small, the comprehensive performance of MC-OTR4 is better than that of MC-ATR4. This is because under the condition of the same cross-sectional area of the groove, the depth of the triangular groove decreases further. Microchannels with staggered triangular grooves exhibit a flow mechanism similar to waves. The direction of the main flow line

changes periodically, the pressure drop of the microchannel decreases, and the flow resistance of the fluid decreases. Although its heat transfer performance is worse than that of the contralateral grooves, its comprehensive performance is higher due to its low flow resistance.
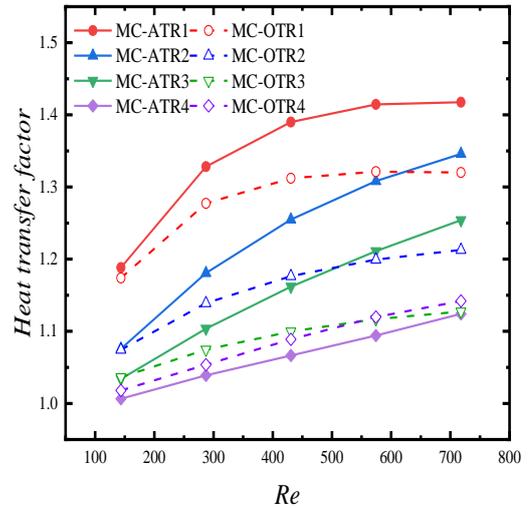

Figure 9: Comprehensively strengthen the change of heat transfer factor
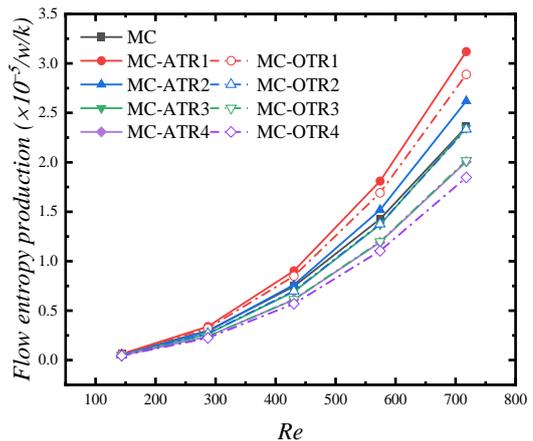
D. Entropy generation analysis
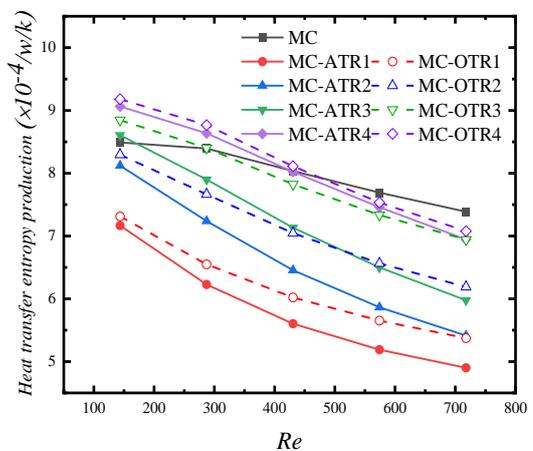

Figure 10:Change inflow entropy production

Figure 11: Change in heat transfer entropy production

Fig. 10 shows the changes in friction entropy production of microchannels at different Reynolds numbers. The friction entropy production number of the microchannel increases with the increase of Re, because with the increase of Re, the friction resistance of the channel also increases, and the irreversible loss

caused by the friction resistance also increases.The friction entropy production of MC-ATR1 is the largest, and that of MC-OTR4 channel is the smallest. The friction entropy production of MC-ATR1, MC-OTR1 and MC-ATR2 channels is greater than that of smooth surface microchannels. The friction entropy production of other channels with grooves is smaller than that of smooth channels.The friction entropy production of the staggered triangular grooves microchannel is smaller than that of the opposite row triangular grooves microchannel.

It can also be seen from Fig. 10 and Fig. 11 that the entropy yield caused by the irreversibility of heat transfer is much higher than that caused by the irreversibility of flow friction, indicating that the irreversible loss of heat transfer dominates the total entropy yield.This is because the geometric size of the microchannel is small, the fluid velocity is low, and the irreversible loss caused by flow friction has a small effect on the total entropy yield. Therefore, the total entropy yield is mainly affected by the heat transfer entropy yield in the process of the microchannel fluid flow and heat transfer enhancement.

Fig. 12 shows the change of the increase of the total entropy production of the channel under different Reynolds numbers.The increasing number of entropy production of microchannels decreases with the increase of Re, and the decreasing degree becomes slow gradually.Except for the channels MC-ATR3, MC-ATR4, MC-OTR3 and MC-OTR4, the increase of entropy production of the other channels with grooves is smaller than that of the channels with smooth surfaces.The irreversible loss of flow and heat transfer in MC-ATR1 channel is the smallest, and that in MC-OTR4 channel is the largest.From the perspective of groove arrangement, the increase of the total entropy production of the staggered triangular groove microchannel is larger than that of the opposite row triangular groove microchannel. MC-OTR1 relative to MC-ATR1, MC-OTR2 relative to MC-ATR2, M-OTR3 relative to MC-ATR3 and MC-OTR4 relative to the MCS-ATR4number of entropy production increase were increased 5.89×10^{-2}、9.82×10^{-2}、1.22×10^{-1} and 1.50×10^{-2}.
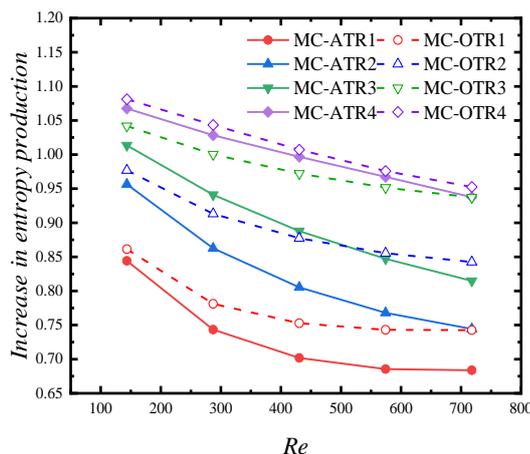

Figure 12:Change in the increase in entropy production

CONCLUSION

(1)When the volume of the channel is the same, the flow resistance of the microchannel increases with the increase of groove depth and groove width.Compared with the smooth surface microchannel, the maximum pressure drop increment of the microchannel in the aligned and staggered triangular grooves is 33.38kPa and 31.45kPa, respectively.

(2)On the one hand, the groove structure increases the volume of the flow passage, reduces the flow velocity and reduces the flow resistance. On the other hand, the mixing of the fluid is strengthened, and the reverse pressure gradient is formed in the flow passage, which increases the flow resistance.

(3)When the flow channel volume is the same, the heat transfer performance of the microchannel increases with the increase of groove depth and the decrease of groove width. The heat transfer performance of the microchannel with the opposite groove is better than that of the staggered groove microchannel.MC-ATR1 has the largest flow pressure drop and relative Nusselt number, as well as the best overall performance.

(4)The entropy production rate caused by irreversible heat transfer is much higher than that caused by irreversible flow friction, and the irreversible loss of flow and heat transfer in MC-ATR1 channel is the least.

References

[1] D.,B.T. and F.W.P. R., High-performance heat sinking for VLSI. IEEE Electron Device Letters, 1981. 2(5): p. 126-129.

[2] Wang. H., Z. Chen and J. Gao, Influence of geometric parameters on flow and heat transfer performance of micro-channel heat sinks. Applied Thermal Engineering, 2016. 107: p. 870-879.

[3] Yue. Y., S.K. Mohammadian and Y. Zhang, Analysis of performances of a manifold microchannel heat sink with nanofluids. International Journal of Thermal Sciences, 2015. 89: p. 305-313.

[4] Ahmed, H.E. and M.I. Ahmed, Optimum thermal design of triangular, trapezoidal and rectangular grooved microchannel heat sinks. International Communications in Heat and Mass Transfer, 2015. 66: p. 47-57.

[5] Zhu. Q., Fluid flow and heat transfer characteristics of microchannel heat sinks with different groove shapes. International Journal of Thermal Sciences, 2021. 161: p. 106721.

[6] D., A., H. A. and K. K., Multiobjective Optimization of a Grooved Micro-Channel Heat Sink. IEEE Transactions on Components and Packaging Technologies, 2010. 33(4): p. 767-776.

[7] Bar-Cohen, A., A.D. Kraus and P.A. Engel, Advances in Thermal Modeling of Electronic Components and Systems, Vol. 1. Journal of Electronic Packaging, 1989. 111(2): p. 162-162.

[8] Xia, G.D., et al., Effects of different geometric structures on fluid flow and heat transfer performance in microchannel heat sinks. International Journal of Heat and Mass Transfer, 2015. 80: p. 439-447.

[9] Steinke, M.E. and S.G. Kandlikar, Single-phase liquid friction factors in microchannels. International Journal of Thermal Sciences, 2006. 45(11): p. 1073-1083.

[10] Chambrepaul, A., Flow of Rarefied Gases. 1961: Flow of Rarefied Gases.

[11] Incropera, F.P., Liquid Cooling of Electronic Devices by Single-phase Convection. mechanical engineering, 1999. 36(4): p. 615-626..

[12] Webb, R.L., Performance evaluation criteria for use of enhanced heat transfer surfaces in heat exchanger design. International Journal of Heat and Mass Transfer, 1981. 24(4): p. 715-726.

[13] Bejan, A., Entropy Generation Through Heat and Fluid Flow. Wiley, 1982.

[14] Shah and K. R., Laminar Flow Forced Convection in Ducts. 1978: p. 366-384.

[15] Zhou, J., X. Chen and Q. Li, Numerical study on two-phase boiling heat transfer performance of interrupted microchannel heat sinks. Science China Technological Sciences, 2022. 65(3): p. 679-692.